Electronic Supplementary Material (ESI) for Nanoscale.

Electronic Supplementary Information (ESI†) for "Large magneto-optical effects in hole-doped blue phosphorene and gray arsenene"

Xiaodong Zhou, Wanxiang Feng,* Fei Li, and Yugui Yao*
Beijing Key Laboratory of Nanophotonics and Ultrafine Optoelectronic Systems,
School of Physics, Beijing Institute of Technology, Beijing 100081, China

Corresponding authors: (W.F.) wxfeng@bit.edu.cn; (Y.Y.) ygyao@bit.edu.cn

TABLE S1. The calculated lattice constants a_0, sublattice heights h, interlayer distances Δ, effective thicknesses (d), relativistic band gaps E_g for monolayer (ML) and bilayers (AA, AB, and AC stacking configurations) phosphorene, arsenene, and antimonene with buckled crystal structure. δE are the energy variations between different bilayers with respect to AA stacking. The relevant theoretical and experimental results are listed for comparisons.

	a_0 (Å)	h (Å)	Δ (Å)	d (Å)	E_g (eV)	δE (meV)
P-ML	3.278	1.237	-	4.580	1.932	-
	3.326[a]	1.230[b]	-	-	2.000[a],1.940[c]	-
	3.675[d]	1.180[d]	-	-	1.100[d]	-
P-AA	3.275	1.245	4.529	9.059	1.127	0.0
	-	1.240[c]	4.470[b,c]	-	1.000[c]	-
P-AB	3.276	1.245	4.521	9.043	1.119	2.2
	-	1.240[c]	4.440[b,c]	-	0.970[c]	2.0[c]
P-AC	3.274	1.245	4.690	9.379	1.232	0.0002
	-	1.240[c]	4.650[c]	-	1.140[c]	0.1[c]
As-ML	3.609	1.398	-	4.455	1.480	-
	3.607[e]	1.388[e]	-	-	1.635[e],1.710[f]	-
	3.601[g]	1.394[g]	-	-	1.460[h],1.480[g]	-
As-AA	3.600	1.407	4.516	9.031	0.790	0.0
	3.620[f]	-	4.310[f]	-	-	-
	3.610[h]	1.400[h]	4.670[h]	-	0.700[h]	-
As-AB	3.616	1.402	4.295	8.597	0.569	2.5
As-AC	3.606	1.404	4.550	9.101	0.791	4.3
Sb-ML	4.121	1.645	-	4.616	0.998	-
	4.122[g]	1.640[g],1.570[i]	-	-	1.000[g]	-
Sb-AA	4.102	1.660	4.745	9.491	0.288	0.0
	-	1.500[j]	3.800[j]	-	-	-
Sb-AB	4.133	1.651	4.435	8.870	0.161	-11.1
	4.280[i]	1.570[i]	3.730[i]	-	-	-
Sb-AC	4.127	1.647	4.666	9.332	0.275	5.2

[a] Ref. [1] (GGA-PBE), [b] Ref. [2] (GGA-PBE & DFT-vdW), [c] Ref.[3] (GGA-PBE & DFT-D2), [d] Ref. [4] (Experiment), [e] Ref. [5] (GGA-PBE), [f] Ref. [6] (GGA-PBE & DFT-optB86b-vdw), [g] Ref. [7] (GGA-PBE & SOC), [h] Ref. [8] (GGA-PBE & SOC & DFT-vdw), [i] Ref. [9] (Experiment), [j] Ref. [10] (Experiment).

TABLE S2. Largest Kerr and Faraday rotation angles for typical magneto-optical materials, including 3*d*-transition-metal/noble-metal multilayers (Fe/Cu, Fe/Au, and Co/Au) and 3*d*-transition-metal compound thin films (MnBi and $Y_3Fe_5O_{12}$).

	θmax K (deg)	$\hbar\omega_K$ (eV)	θmax F (10^5 deg/cm)	$\hbar\omega_F$ (eV)
Fe/Cu[a]	0.06	2.21	-	-
Fe/Au[b]	0.16	2.50	-	-
Co/Au[c]	0.06	1.96	-	-
MnBi[d]	2.3	1.82	7.96	1.77
$Y_3Fe_5O_{12}$[e,f]	0.23	2.95	0.02	2.07

[a] Ref. [11], [b] Ref. [12], [c] Ref. [13], [d] Ref. [14], [e] Ref. [15], [f] Ref. [16]

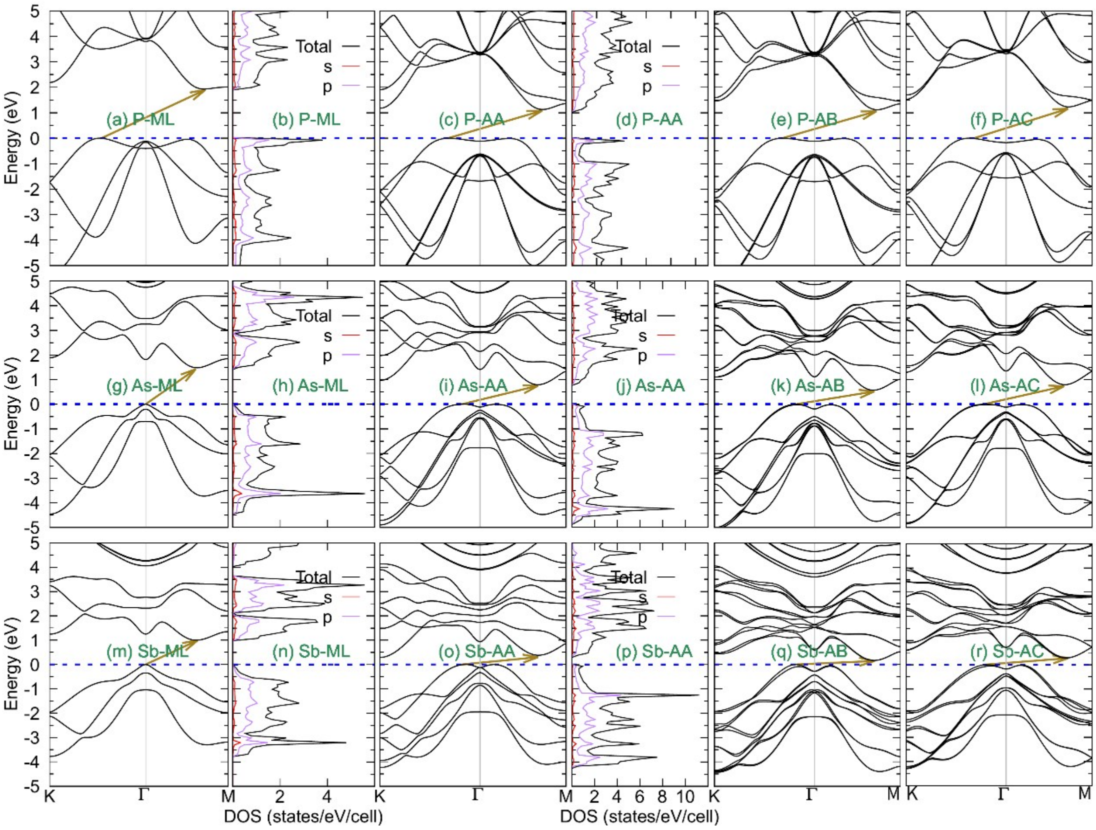

FIG. S1. (a)(g)(m) Relativistic band structures of monolayer (ML) phosphorene, arsenene, and antimonene with buckled crystal structure. (b)(h)(n) The corresponding density of states. (c)(i)(o) Relativistic band structures of bilayer phosphorene, arsenene, and antimonene with AA stacking configuration. (d)(j)(p) The corresponding density of states. (e)(k)(q) and (f)(l)(r), relativistic band structures for bilayers phosphorene, arsenene, and antimonene with AB and AC stacking configurations, respectively. The density of states for AB and AC configurations are not shown because of the similarity with AA configuration. The Fermi levels, indicating by blue dashed lines, are set to the valence band maximums. The indirect band gaps are indicated by yellow arrows.

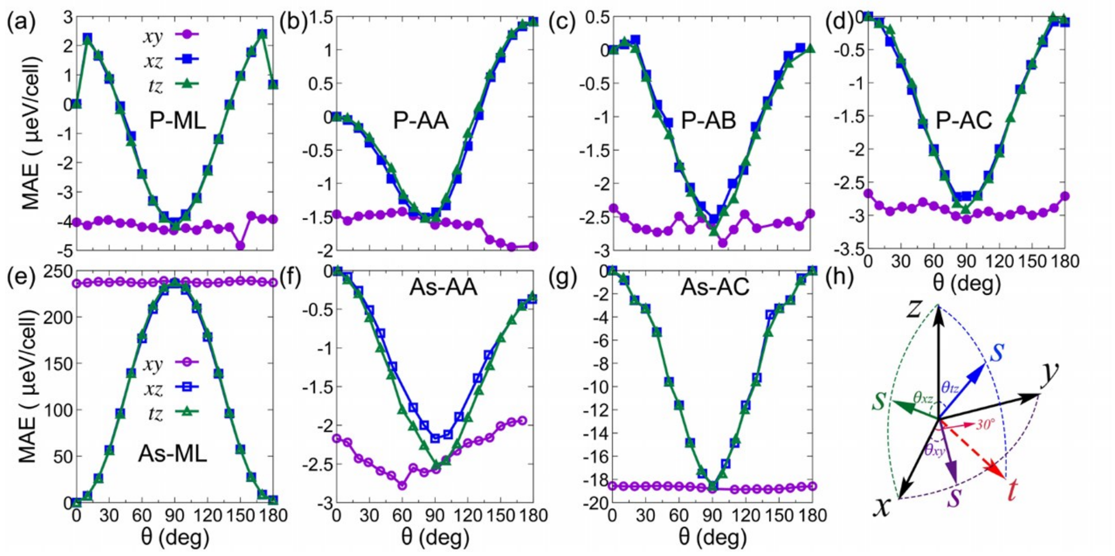

FIG. S2. (a)-(g) Magnetocrystalline anisotropic energy (MAE) of monolayer and bilayers blue phosphorene and gray arsenene at critical hole-doping concentrations p_m. The spin direction is rotated from 0 to π on three different planes, *xy*, *xz*, and *tz*, shown in (h), where *t*-axis is the angle bisector of crystal vectors. Here, the MAE is defined as the energy difference between the spin polarization pointing to an arbitrary direction and the out-of-plane (i.e., the [001]) direction. In blue phosphorene, the in-plane spin polarization has the lower energy for both monolayer and bilayers. While in gray arsenene, monolayer and bilayers prefer the out-of-plane and in-plane spin polarizations, respectively. The MAE of gray arsenene is significantly larger than that of blue phosphorene, epically for the monolayer (more than two orders of magnitude). In addition, AA-stacked bilayers blue phosphorene and gray arsenene exhibit significantly asymmetric MAE when the spin points to above and below the xy plane, due to the lacking of crystalline mirror symmetry along the z-axis. Monolayers and AB-stacked bilayers of blue phosphorene and gray arsenene also show asymmetric MAE but the magnitudes are too small.

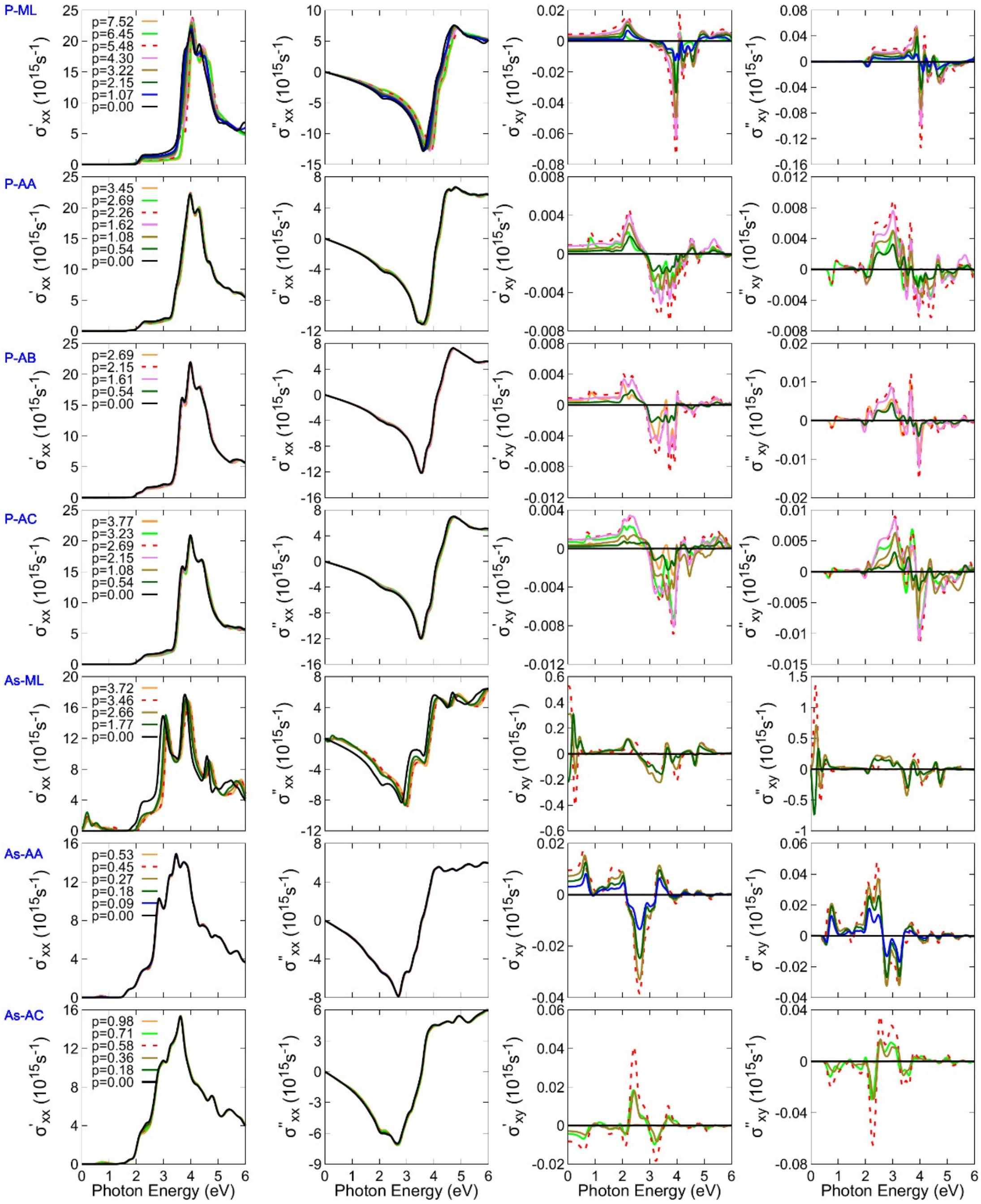

FIG. S3. Optical conductivities of monolayer and bilayers blue phosphorene and gray arsenene under different hole-doping concentrations (p is in the unit of 10^{14} cm^{-2}). The spin is polarized along the [001] direction (i.e., the z-axis). The dashed lines represent the optical conductivities at the critical doping concentrations p_m.

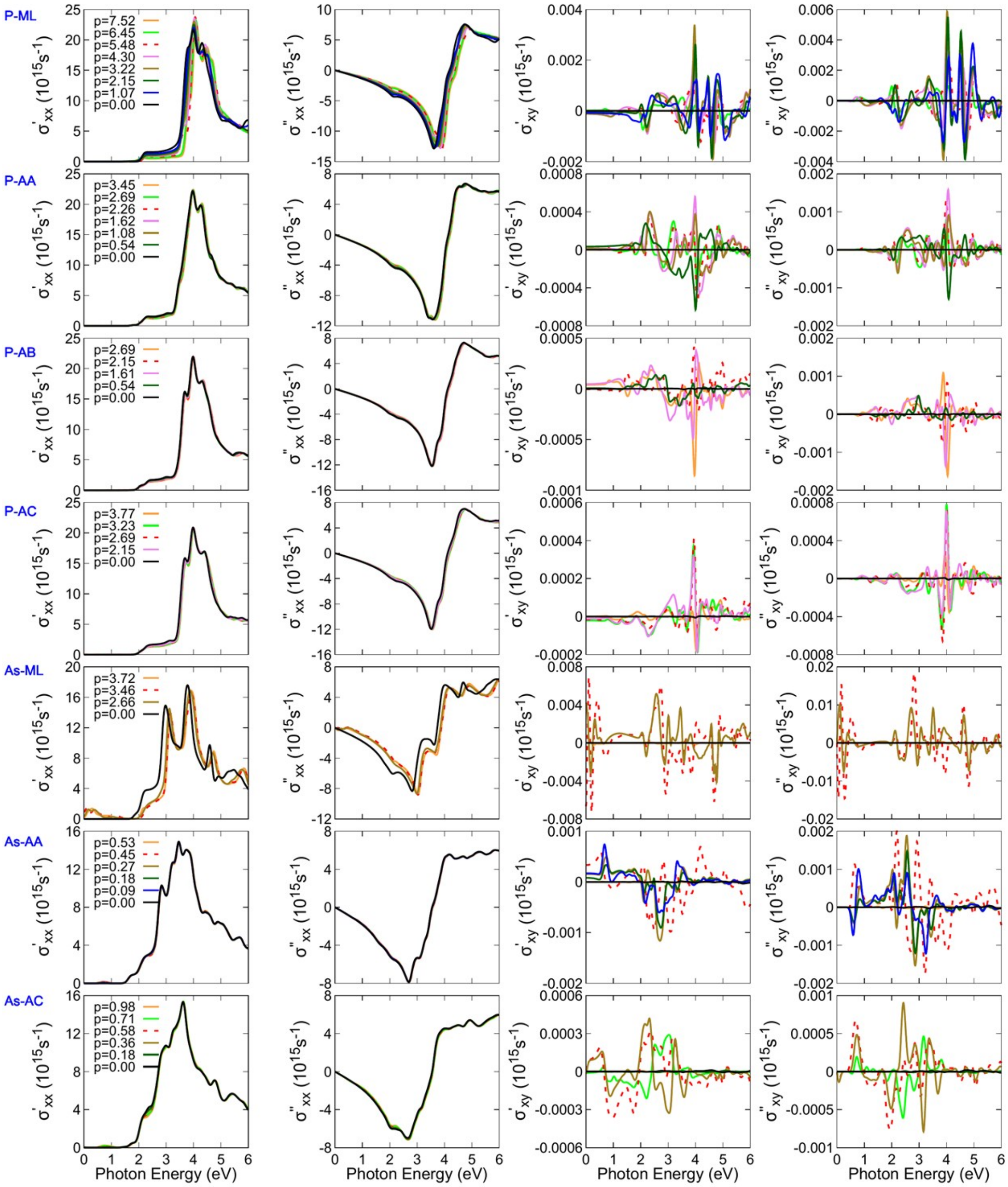

FIG. S4. Optical conductivities of monolayer and bilayers blue phosphorene and gray arsenene under different hole-doping concentrations (p is in the unit of 10^{14} cm^{-2}). The spin is polarized along the [100] direction (i.e., the x-axis). The dashed lines represent the optical conductivities at the critical doping concentrations p_m.

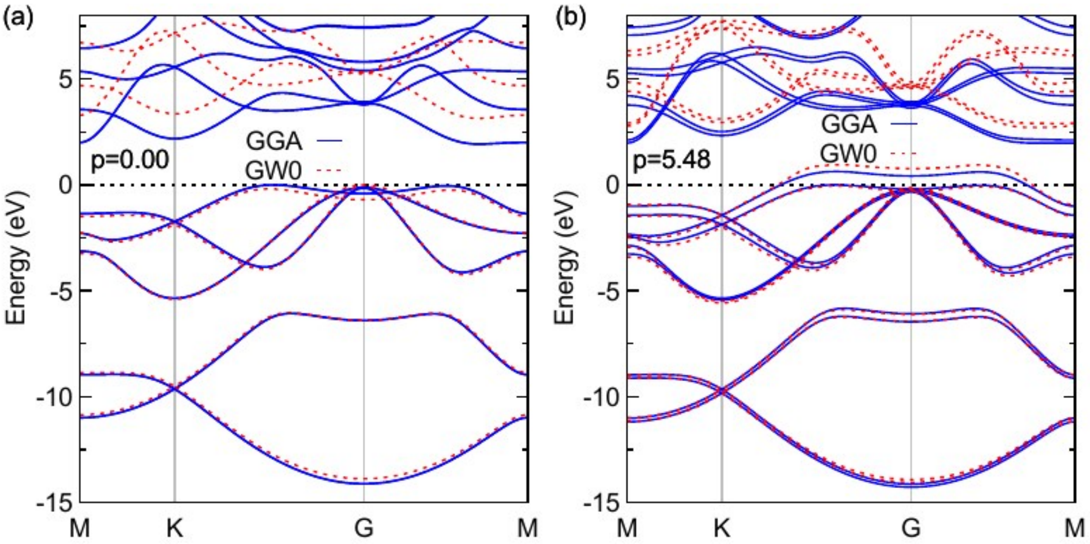

FIG. S5. Band structures of monolayer blue phosphorene at zero (a) and critical (b) hole doping. The unit of doping concentration is 10^{14} cm^{-2}. For the GW$_0$ calculation, the energy cutoff of 350 eV and the Monkhorst-Pack k-mesh of $13 \times 13 \times 1$ are adopted.

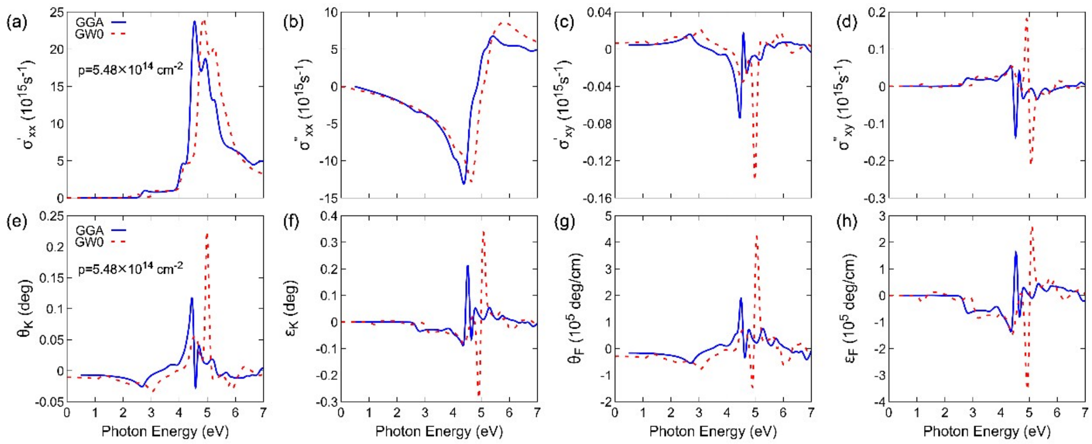

FIG. S6. Optical and magneto-optical spectra of monolayer blue phosphorene at the critical hole concentration (p=5.48×10^{14} cm^{-2}). The GGA lines are shifted 0.49 eV by acting on the scissor operator.

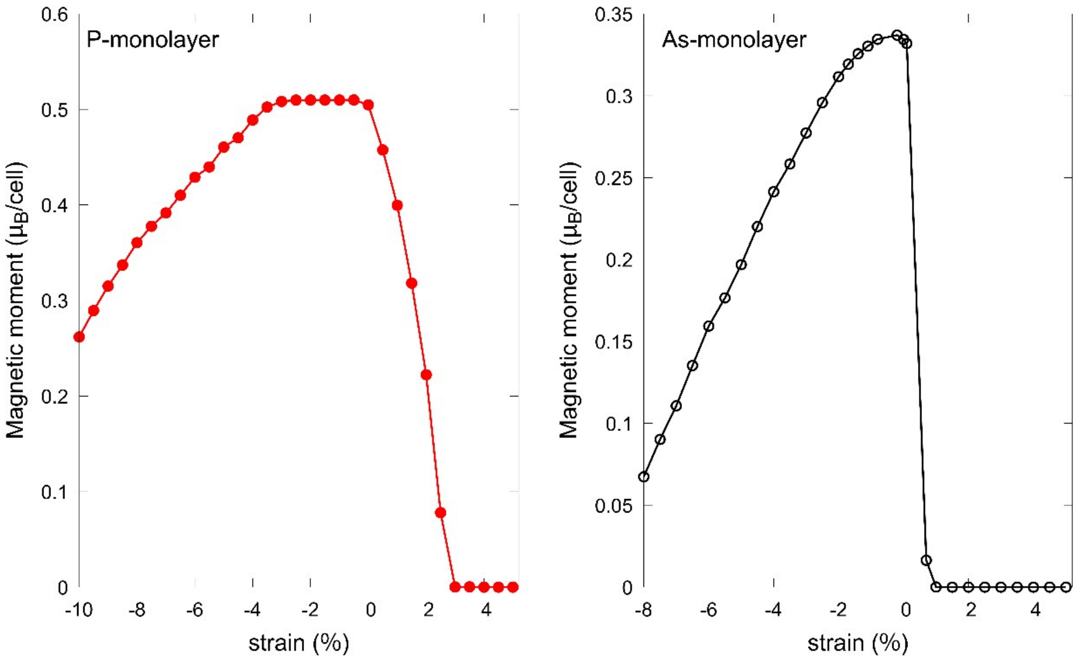

FIG. S7. Spin magnetic moments of monolayer blue phosphorene and gray arsenene as a function of biaxial strains with 0.51 hole per cell ($p = 5.48 \times 10^{14}$ cm^{-2}) and 0.39 hole per cell ($p = 3.46 \times 10^{14}$ cm^{-2}), respectively. The calculations are included the spin-orbit coupling.

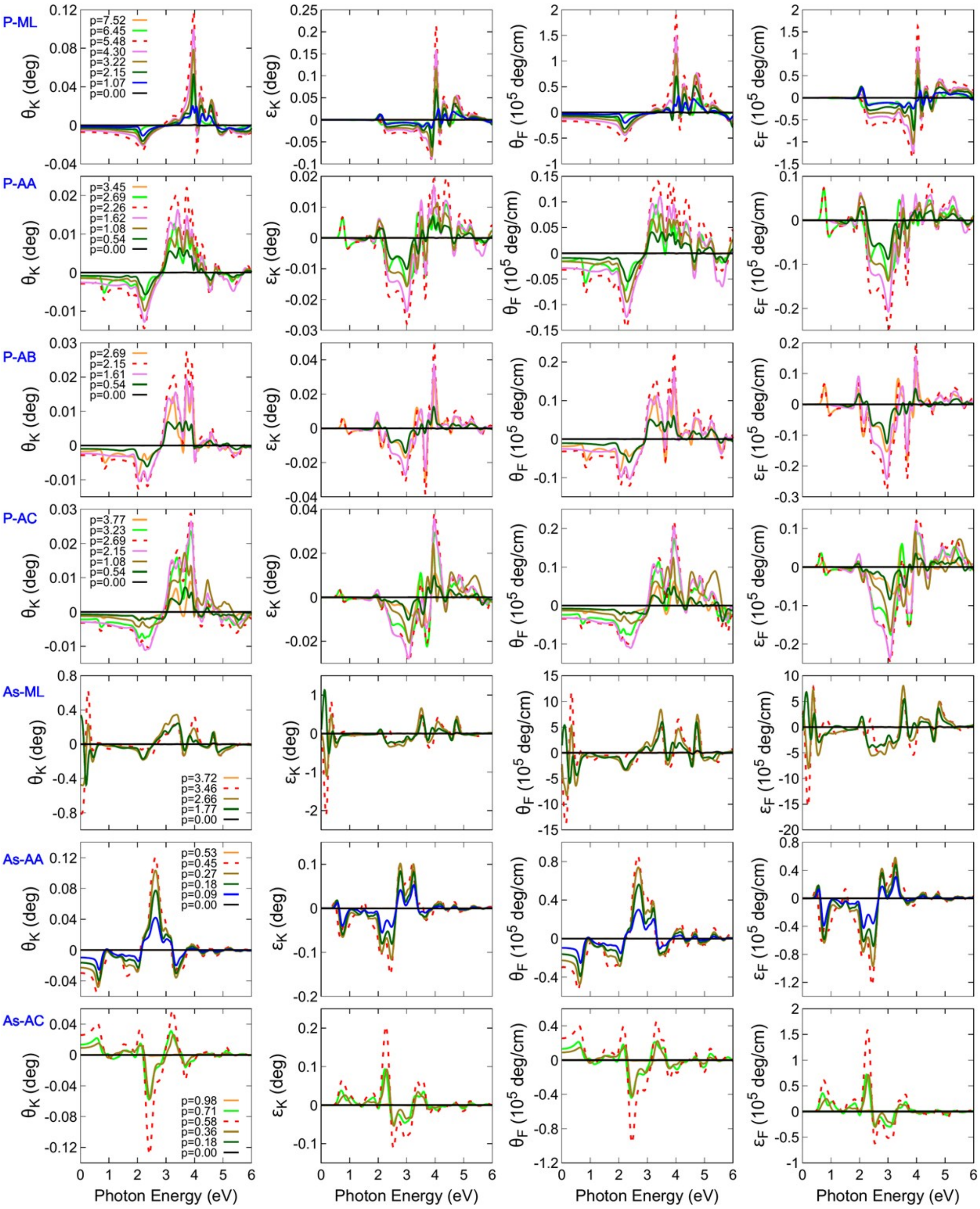

FIG. S8. Magneto-optical spectra of monolayer and bilayers blue phosphorene and gray arsenene under different hole-doping concentrations (p is in the unit of 10^{14} cm^{-2}). The spin is polarized along the [001] direction (i.e., the z-axis). The dashed lines represent the magneto-optical spectra at the critical doping concentrations p_m.

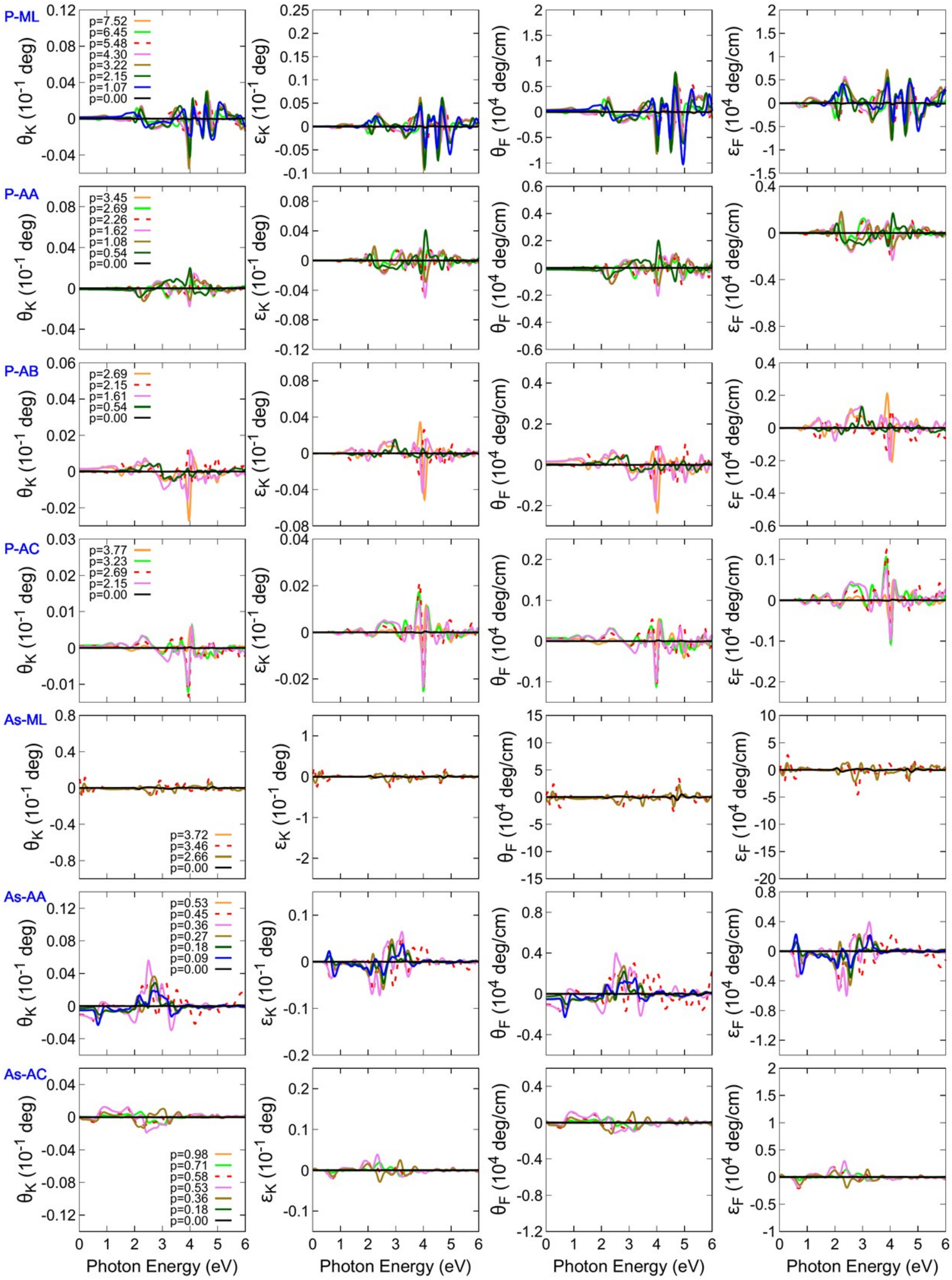

FIG. S9. Magneto-optical spectra of monolayer and bilayers blue phosphorene and gray arsenene under different hole-doping concentrations (p is in the unit of 10^{14} cm^{-2}). The spin is polarized along the [100] direction (i.e., the x-axis). Note that the units of Kerr and Faraday spectra are one order of magnitude smaller than that used in Fig. S6. The dashed lines represent the magneto-optical spectra at the critical doping concentrations p_m.

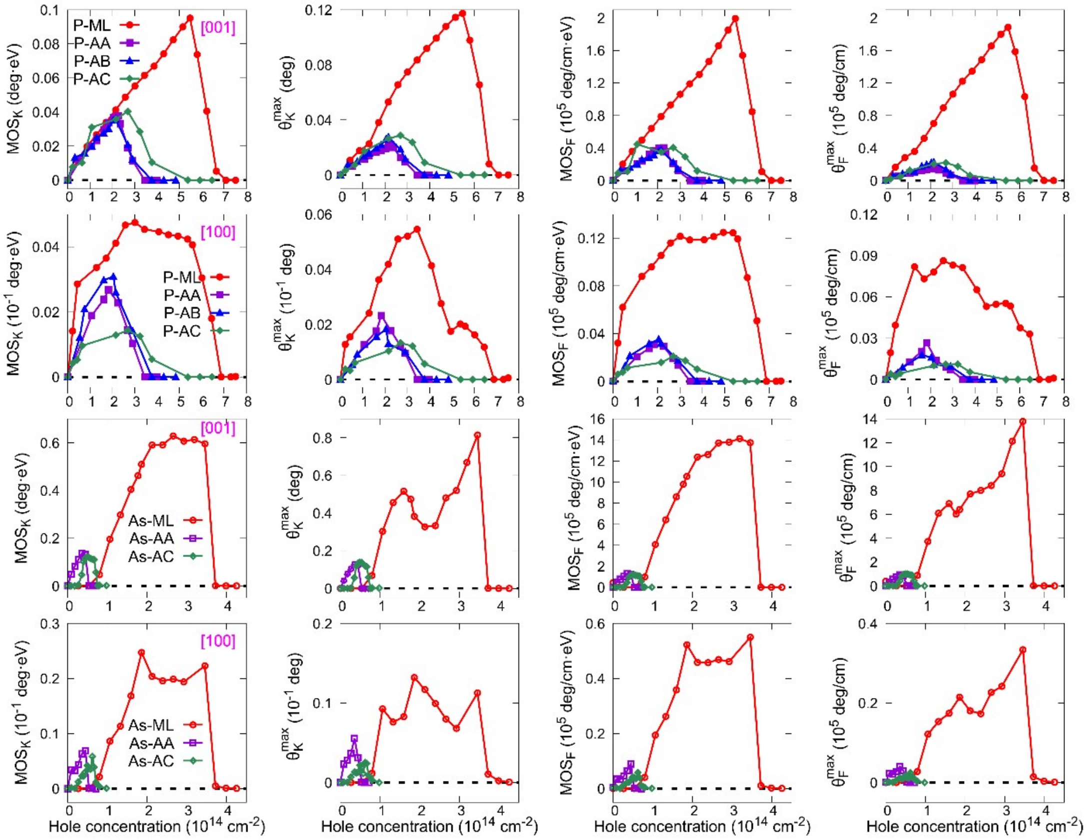

FIG. S10. Magneto-optical Kerr and Faraday strength (MOS$_K$ and MOS$_F$) and the maximums of Kerr and Faraday rotation angles (*θmax K*and *θmax F*) in monolayer and bilayers blue phosphorene and gray arsenene as a function of hole-doping concentration. The results of in-plane spin polarization are at least one order of magnitude smaller than those of out-of-plane spin polarization.

References:

[1] Z. Zhu and D. Tománek, Phys. Rev. Lett. 112, 176802 (2014).

[2] Y. Mogulkoc, M. Modarresi, A. Mogulkoc, and Y. O. Ciftci, Comput. Mater. Sci. 124, 23 (2016).

[3] B. Ghosh, S. Nahas, S. Bhowmick, and A. Agarwal, Phys. Rev. B 91, 115433 (2015).

[4] J. L. Zhang, S. Zhao, C. Han, Z. Wang, S. Zhong, S. Sun, R. Guo, X. Zhou, C. D. Gu, K. D. Yuan, and et al., Nano Lett. 16, 4903 (2016).

[5] C. Kamal and M. Ezawa, Phys. Rev. B 91, 085423 (2015).

[6] Z. Zhu, J. Guan, and D. Tománek, Phys. Rev. B 91, 161404(R) (2015).

[7] G. Pizzi, M. Gibertini, E. Dib, N. Marzari, G. Iannaccone, and G. Fiori, Nat. Commun. 7, 12585 (2016).

[8] D. Kecik, E. Durgun, and S. Ciraci, Phys. Rev. B 94, 205409 (2016).

[9] P. Ares, F. Aguilar-Galindo, D. Rodríguez-San-Miguel, D. A. Aldave, S. Díaz-Tendero, M. Alcamí, F. Martín, J. Gómez-Herrero, and F. Zamora, Adv. Mater. 28, 6332 (2016).

[10] J. Ji, X. Song, J. Liu, Z. Yan, C. Huo, S. Zhang, M. Su, L. Liao, W. Wang, Z. Ni, Y. Hao, and H. Zeng, Nat. Commun. 7, 13352 (2016).

[11] T. Katayama, Y. Suzuki, H. Awano, Y. Nishihara, and N. Koshizuka, Phys. Rev. Lett. 60, 1426 (1988).

[12] Y. Suzuki, T. Katayama, S. Yoshida, K. Tanaka, and K. Sato, Phys. Rev. Lett. 68, 3355 (1992).

[13] R. Mégy, A. Bounouh, Y. Suzuki, P. Beauvillain, P. Bruno, C. Chappert, B. Lecuyer, and P. Veillet, Phys. Rev. B 51, 5586 (1995).

[14] G. Q. Di and S. Uchiyama, Phys. Rev. B 53, 3327 (1996).

[15] S. Tomita, T. Kato, S. Tsunashima, S. Iwata, M. Fujii, and S. Hayashi, Phys. Rev. Lett. 96, 167402 (2006).

[16] T. Boudiar, B. Payet-Gervy, M.-F. Blanc-Mignon, J.-J. Rousseau, M. L. Berre, and H. Joisten, J. Magn. Magn. Mater. 284, 77 (2004).